The internal calcar septum and its contact with the virtual stem in THR

A computer tomographic evaluation

Jens Decking[1], Ralf Decking[2], Carsten Schoellner[1], Philipp Drees[1] and Anke Eckardt[1]

Departments of Orthopaedic Surgery, [1]University of Mainz, [2]University of Ulm, Germany
Correspondence: decking@mail.uni-mainz.de
Submitted 02-05-07. Accepted 03-01-09

ABSTRACT The internal calcar septum is a ridge of cortical bone protruding from the inner cortical wall of the proximal femur into the medullary canal. It extends from the lesser trochanter into the femoral neck and narrows the femoral cavity in its dorsal third. This region is essential for THR stability, but the degree of contact between the septum and standard THR implants has never been studied.

We obtained CT scans of 50 arthrotic hip joints from patients requiring THR. Virtual stems (50 straight/wedge-shaped and 50 anatomic stems) were placed in CT images of the femora using a PC-based preoperative planning unit. The dimensions of the septum, degree and location of contact between the septum and implants were recorded.

A septum of cortical density was seen in 49/50 CT scans. It was 11 (2.9) mm long (medial-lateral), 3.5 (0.7) mm wide and 32 (10) mm high (caudal-cranial, mean (SD)). 94/100 implanted virtual stems showed direct contact with the septum. 31 straight stems and 5 anatomical stems were supported by the septum along their dorsal side.

The internal calcar septum can be consistently seen on CT scans of patients needing THR and it probably contributes to THR stability.

The internal calcar septum is a ridge of cortical bone protruding from the dorsomedial endosteal cortex into the medullary canal. It extends from the lesser trochanter into the femoral neck, narrowing the dorsal part of the main femoral cavity (Dai et al. 1985). The septum was mentioned by Merkel in 1874 and described in much the same way in contemporary CT studies of the proximal femur (Brown and Ferguson 1980, Dai et al. 1985, Walker and Robertson 1988, Laine et al. 2000). In a recent anatomic and radiographic study by Adam et al. (2001), the internal calcar septum was reported to be a ridge of cortical density, up to 3 mm thick and 35 mm long, connected in all parts with the surrounding cancellous bone in the metaphysis of the proximal femur.

This ridge is located in a region essential for support and primary stability of cementless THR stems. In experimental studies, Callaghan et al. (1992) and Dujardin et al. (1996) showed that fit and fill of stems in the metaphyseal region correlated with the initial rotational and vertical stability of the implants. Nunn et al. (1989) found that rotational stability of the stem is significantly increased by cortical contact between the stem and the femoral neck. Thus, the calcar septum may contribute to primary stability of cementless stems or affect their positioning during manual broaching of the femoral canal. In a series of CT-based virtual stem implantations, we evaluated the degree of contact achieved between the calcar septum and standard cementless stems of anatomical or straight design.

Material and methods

Patients and robotic-assisted THR

CT scans of the proximal femur were obtained

from 50 consecutive patients (27 men), who underwent cementless THR with robotic-assisted reaming of the femoral canal during 2000–2001. 45 patients had primary osteoarthrosis of the hip and 5 had femoral head necrosis. Their mean age was 54 (35–64) years. In robotic-assisted THR, CT scans of the affected hip joints form the basis of preoperative planning. CT images are transferred into PC-based planning software. Virtual implants are placed in the CT images, and a robot reams the femoral canal, according to the preoperative planning (Bargar et al. 1998, Nogler et al. 2001).

CT examinations

Preoperative CT was done with a Siemens Somatom Plus 4 scanner (Siemens Medical Division, Erlangen, Germany). From the femoral head to the base of the greater trochanter, the scan parameters were 2 mm slice collimation and 3 mm feed per rotation (140kV/171mA). From the base of the greater trochanter to the diaphysis, we used 3 mm slice collimation and 4.5 mm feed per rotation (140kV/129mA). The field of view was set at 200–250 mm; CT images were reconstructed with a pixel matrix of 512 × 512.

Image analysis software and virtual stem implantation

The preoperative planning unit Torch (URS-ortho, Rastatt, Germany) displays CT images of the femur in the frontal, lateral, and transverse views simultaneously. The surgeon selects different types and appropriate sizes of stems from a menu and places the virtual implant in the CT image of the femur by mouse-control (Figure 1). The virtual implant head is placed at the predicted height of the rotational center of the acetabular component, as estimated from the CT images, usually the midpoint of the greatest diameter of the acetabulum in the frontal view. If preoperative leg-length inequality is present, the implant head should be placed more cranially or caudally, as needed. The anteversion of the implant neck is adjusted to reconstruct the anatomical antetorsion of the femoral neck, with a target value of 10–25°.

In each of the 50 CT scans, two stem designs were placed: one was straight, narrow and wedge-shaped (CBC, Mathys, Switzerland), the other had an anatomical shape (G2, ESKA Implants, Germany). The latter is, in fact, slightly fuller and broader in the metaphyseal region than a real anatomical stem, but it is called "anatomical" in this study for simplicity's sake. Each implant was individually placed to obtain an optimum fit and fill in the medullary canal and the best combination of stem-size, leg-length, anteversion, and alignment of femoral and stem axes.

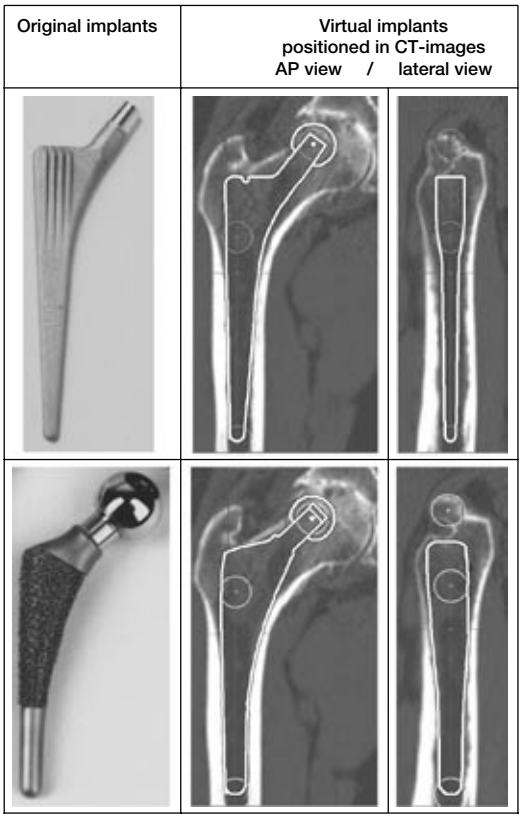

Figure 1. The Mathys CBC stem (top row) is straight and wedge-shaped, and has a narrow rectangular cross-section. The ESKA G2 stem (bottom row) has a broad anatomical shape and an oval cross section. The resulting differences in fit-and-fill and in the cortical contact areas are seen in the CT-based preoperative planning unit (Torch, URS-ortho) in the right and middle columns.

Analysis of the internal calcar septum and implantation parameters

The most dorsomedial point of the lesser trochanter defined the lesser trochanter level (Figure 2). The extension of the internal cortical septum from this level in proximal and distal directions was recorded. The merging of the septum with the cortex of the dorsomedial neck proximally and the

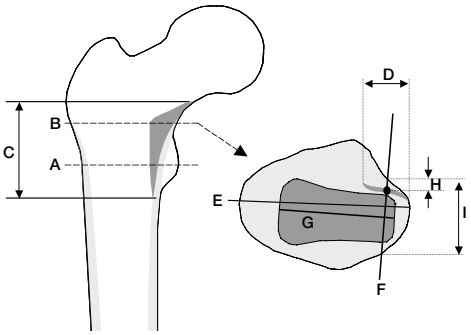

Figure 2. Measurements of the calcar septum were done in the transverse plane (right side) at the level of the greatest length of the septum (B, left side).
A. lesser trochanter level
B. level of greatest septum length
C. height of septum in proximal/distal direction
D. length of septum in medial/lateral direction
E. longest oblique diameter of the femoral canal
F. line through septum's midpoint
G. stem-neck line
H. distance between septum midpoint and dorsal cortex
I. width of the femoral cavity

lower border of the lesser trochanter distally were defined as endpoints of the septum. Next, the greatest length of the calcar septum in a medio-lateral direction was determined in transverse CT sections (Figure 2, right side). The distance of the lesser trochanter level to the level of greatest septum length was recorded. All of the following parameters were measured at the level of the greatest septum length. The longest oblique diameter of the femoral cavity was measured and its correlation to the septum length was calculated. The midpoint of the spur was determined and its density (HU) recorded. A line through the septum's midpoint and perpendicular to the stem-neck line was drawn. Distances from the midpoint of the septum to the dorsal endosteal border of the femoral cavity, the width of the femoral cavity and that of the septum were measured along this line. The length of the contact area between the virtual implant and the calcar septum was measured. The location of contact between the virtual implant and the calcar septum was described as dorsal, medial, or dorsomedial to the implant or without contact (Figure 3).

To determine the cortical borders of the femoral canal and the dimensions of the internal calcar septum along the cross-sections described above, we used the "50% relative threshold (RT50)" method, described by Prevrhal et al. (1999). Whenever this method was not applicable because of high density of spongious bone or inhomogeneous scattering of HU in the vicinity of the calcar septum, a fixed threshold of 400 HU was regarded as the cortical border.

The anteversion of the stem-neck line is computed automatically by the Torch preoperative planning unit with reference to the tangent to the most dorsal points of the lateral and medial femoral epicondyle (Waidelich et al. 1992). We also measured the distance from the line of neck resection, as shown in the planning unit, to the level of the lesser trochanter.

Statistics

Pearsons Linear Correlations was used to determine the correlation of the greatest septum length with the longest oblique diameter of the femoral cavity and to correlate the position of the septum's midpoint with the dorso-ventral endosteal diameter

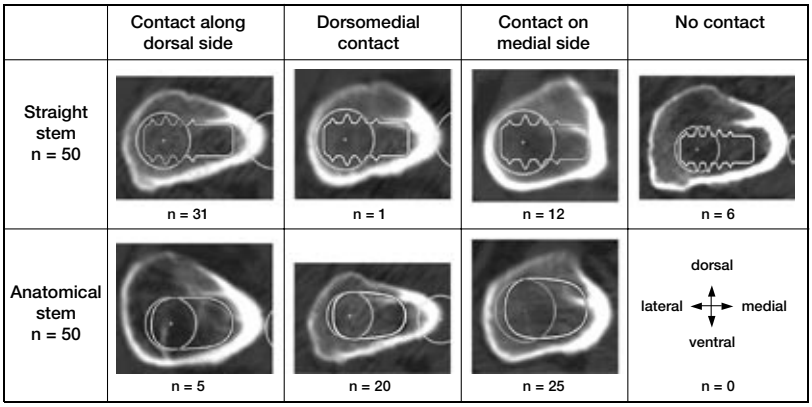

Figure 3. Location of contact between the internal calcar septum and the implants in transverse CT sections at the level of the greatest septum length.

of the femoral cavity. The Student's t-test was used to evaluate differences between implant-specific parameters (length of contact between the implant and septum).

Results

The internal calcar septum was visible in 49 CT scans, but not in 1 case. Its length and range in the medio-lateral direction were 11 (2.9) mm (mean (SD)), 5–19 mm and width at its midpoint were 3.5 (0.7) mm, 2.7–5.6 mm. Its height and range in the caudal-cranial direction were 32 (10) mm, 24–56 mm. When it was measured from the level of the lesser trochanter, it extended 27 (5.7) mm in the cranial direction and 5.1 (9.2) mm in the caudal. The level of its greatest length was located 13 (4.9) mm cranial to the level of the lesser trochanter. The density at its midpoint was 758 (171) HU, ranging from 380 HU to 1010 HU.

The longest oblique diameter of the femoral cavity at the level of the greatest septum-length was 38 (8.5) mm, 29–58 mm. The correlation between the longest oblique diameter of the femoral cavity with the length of the septum was poor (Pearson corr. coeff. = 0.4). The distance between the septum's midpoint and the dorsal endosteal borders of the femoral cavity was 5.9 (1.7) mm; the distance between the dorsal and the ventral endosteal borders of the femoral cavity, measured in the same region, was 20 (3.5) mm. The correlation between these distances was also poor (Pearson corr. coeff. = 0.2).

The number of implants showing dorsal, medial or dorsomedial contact with the calcar septum is shown in Figure 3. The length of the area of contact between the implants and the septum was 5.9 (3.3) mm for all implants. The contact area of the anatomical stem was 4.6 (1.5) mm, as compared to 7.3 (4) mm of the straight stem. The difference in the length of the contact area between the anatomical and straight stems was significant ($p < 0.001$).

The height of the neck resection was 22 (5.6) mm cranial to the lesser trochanter level and anteversion was 16° (5.9°) for all implants. We found no significant difference between the anatomical and straight stems as regards these parameters.

Discussion

The CT scans in this study were obtained under clinical conditions from a typical group of patients who were scheduled to undergo cementless THR surgery. The internal calcar septum was detected in 98% of these cases. It separated the base of the lesser trochanter from the femoral cavity, protruded into the dorsal third of the calcar region in a medio-lateral direction, and finally merged with the dorsomedial cortex in the area of the head-neck junction.

It is important to recognize the limitations of CT-based measurements of thin cortical structures. These measurements are affected by beam-hardening, partial volume effect, CT resolution, and choice of HU thresholding (Sumner et al. 1989, Aamodt et al. 1999). CT-based measurements of the internal femoral canal have an accuracy of 0.8-1.1 mm (Rubin et al. 1992, Laine et al. 1997). With the RT50 method used in this study, Feng et al. (1996) found an accuracy of 0.2 (0.1) mm and Prevrhal et al. (1999) reported an error < 10% if the cortical structures measured on CT are thicker than 0.9 mm. These studies, however, were done under experimental conditions using superior scan parameters. Moreover, there is no anatomically-defined border between the septum and the surrounding cancellous bone: the dense ridge protruding from the calcar cortical wall branches out into trabeculae, merging gradually with the surrounding cancellous bone. Thus, the dimensions of the septum, as described in our study, may be seen as rough coordinates of an irregular structure, representing only the dense cortical stem of the septum.

The correlation between the position of the septum's midpoint and the dorso-ventral internal diameter of the femoral cavity was poor. Moreover, the correlation between the length of the septum and the longest oblique diameter of the femoral cavity was also poor. These findings underline the great variations of the septum, in accord with the studies of Noble et al. (1988) and Laine et al. (2000) who showed that the shape of the proximal femoral medullary canal varied widely in general.

Does the septum contribute to rotational stability of endoprosthetic stems? The stem component of THR is forced into retroversion when a person

walks up stairs and rises from a chair (Nunn et al. 1989, Bergmann 1997). The septum narrows the metaphyseal femoral cavity in its dorsal third and is aligned with the longitudinal axis of the femoral neck (Dai et al. 1985, Laine et al. 2000, Adam et al. 2001). Of 100 virtually-implanted stems, only 6 had no contact with the septum. All of these belonged to the narrow straight stem-type. Nevertheless, the mean length of the area in contact with the septum was greater in straight stems than in anatomical stems. This is because more straight stems are in direct contact with the septum alongside their dorsal aspect, while most anatomic stems meet the septum head-on with its medial face. The virtual stems were implanted in CT images in the approximate position real stems would have assumed in the femur by manual broaching. Therefore, we conclude that a large part of the septum are usually removed by broaching. The shape and position of the septum vary greatly in the femoral canal, and using the septum to maximum advantage will be difficult with hand broaching of the canal and standard implants. If the dense base of the septum is not removed by hand broaching, an increase in the distance between the calcar femoris and the implant's medial face may result. With CT-based preoperative planning, robotic THR or customized implants, on the other hand, the implant can probably be placed against the dense part of the septum.

No competing interests declared.

Aamodt A, Kvistad K A, Andersen E, Lund-Larsen J, Eine J, Benum P, Husby O S. Determination of the Hounsfield value for CT-based design of custom femoral stems. J Bone Joint Surg (Br) 1999; 81: 143-7.

Adam F, Hammer D S, Pape D, Kohn D. The internal calcar septum (femoral thigh spur) in computed tomography and conventional radiography. Skeletal Radiol 2001; 30: 77-83.

Bargar W L, Bauer A, Borner M. Primary and revision total hip replacement using the Robodoc system. Clin Orthop 1998; 354: 82-91.

Bergmann G. In vivo Messung der Belastung von Hueftimplantaten. Koester, Berlin 1997.

Brown T D, Ferguson A B, Jr. Mechanical property distributions in the cancellous bone of the human proximal femur. Acta Orthop Scand 1980; 51: 429-37.

Callaghan J J, Fulghum C S, Glisson R R, Stranne S K. The effect of femoral stem geometry on interface motion in uncemented porous-coated total hip prostheses. Comparison of straight-stem and curved-stem designs. J Bone Joint Surg (Am) 1992; 74: 839-48.

Dai K R, An K N, Hein T J, Nakajima I, Chao E Y. Geometric and biomechanical analysis of the human femur. Orthop Trans 1985; 10: 256.

Dujardin F H, Mollard R, Toupin J M, Coblentz A, Thomine J M. Micromotion, fit, and fill of custom made femoral stems designed with an automated process. Clin Orthop 1996; 325: 276-89.

Feng Z, Ziv I, Rho J. The accuracy of computed tomography-based linear measurements of human femora and titanium stem. Invest Radiol 1996; 31: 333-7.

Laine H J, Kontola K, Lehto M U K, Pitkanen M, Jarske P, Lindholm T S. Image processing for femoral endosteal anatomy detection: description and testing of a computed tomography based program. Phys Med Biol 1997; 42: 673-89.

Laine H J, Lehto M U K, Moilanen T. Diversity of proximal femoral medullary canal. J Arthroplasty 2000; 15: 86-92.

Merkel F. Betrachtungen ueber das Os femoris. Arch Pathol Anat 1874; 59: 237-56.

Noble P C, Alexander J W, Lindahl L J, Yew D T, Granberry W M, Tullos H S. The anatomic basis of femoral component design. Clin Orthop 1988; 235: 148-65.

Nogler M, Krismer M, Haid C, Ogon M, Bach C, Wimmer C. Excessive heat generation during cutting of cement in the Robodoc hip-revision procedure. Acta Orthop Scand 2001; 72: 595-9.

Nunn D, Freeman M A R, Tanner K E, Bonfield W. Torsional stability of the femoral component of hip arthroplasty. Response to an anteriorly applied load. J Bone Joint Surg (Br) 1989; 71: 452-5.

Prevrhal S, Engelke K, Kalender W A. Accuracy limits for the determination of cortical width and density: the influence of object size and CT imaging parameters. Phys Med Biol 1999; 44: 751-64.

Rubin P J, Leyvraz P F, Aubaniac J M, Argenson J N, Esteve P, de Roguin B. The morphology of the proximal femur. A three-dimensional radiographic analysis. J Bone Joint Surg (Br) 1992; 74: 28-32.

Sumner D R, Olson C L, Freeman P M, Lobick J J, Andriacchi T P. Computed tomographic measurement of cortical bone geometry. J Biomech 1989; 22: 649-53.

Waidelich H A, Strecker W, Schneider E. Computertomographische Torsionswinkel- und Laengenmessung an der unteren Extremitaet. RoFo Fortschr Geb Rontgenstr Neuen Bildgeb Verfahr 1992; 157: 245- 51.

Walker P S, Robertson D D. Design and fabrication of cementless hip stems. Clin Orthop 1988; 235: 25-34.